MEASUREMENTS OF THE DYNAMIC STALL VORTEX CONVECTION SPEED

by

R.B. Green, R.A.McD. Galbraith and A.J. Niven,
Department of Aerospace Engineering,
University of Glasgow,
Glasgow,
G12 8QQ,
Scotland.

ABSTRACT

This paper considers the dynamic stall vortex of importance in helicopter rotor aerodynamics and discusses previous measurements of its convection speed. It emerges that an anomaly exists between the available data sets, i.e. that some workers find that the convection speed is dependent upon the aerofoil motion, while others find that this is not the case. Measurements of the convection speed from data gathered at Glasgow University for a variety of aerofoil shapes and motion types are then presented, which support the conclusion that the dynamic stall vortex convection speed is independent of aerofoil type and motion type to a first order.

NOMENCLATURE

AR	model aspect ratio
c	model chord
C_m	pitching moment coefficient (1/4 chord)
C_n	normal force coefficient
f	sampling frequency
h	wind tunnel height
k	reduced frequency ($\omega c/2U$, ω in radian s^{-1})
M	Mach number
r	reduced pitch rate ($\dot{\alpha}c/2U$, $\dot{\alpha}$ in radian s^{-1})
Re	Reynolds number
t	time
U	free stream speed
u	stall vortex convection speed
x	chordwise position
α	incidence
$\dot{\alpha}$	instantaneous pitch rate
$\bar{\alpha}$	mean incidence
$\hat{\alpha}$	amplitude
ω	oscillation frequency

1. INTRODUCTION

To compensate for its reduced airspeed, the retreating blade of a helicopter rotor is pitched up to produce a higher lift coefficient. In steady forward flight, therefore, the blade incidence is continually changing. If the associated pitch rate (or frequency) and pitch amplitude are high enough, dynamic stall will occur. Low speed dynamic stall is characterised by the generation and convection over the blade's suction surface of a powerful vortex structure (the stall vortex) which induces high lift, drag and pitching moment coefficients. Thus, to avoid excessive blade vibrations and to extend the fatigue life, constraints on the flight envelope of the rotor are imposed. Knowledge of the effects of dynamic stall will therefore be required for the structural design of the rotor blade and to predict the behaviour of the rotorcraft.

The passage of the stall vortex over the aerofoil surface influences the aerodynamic coefficients as follows (see figure 1): Vortex growth is accompanied by a rise in the normal force coefficient C_n and a break in the pitching moment coefficient C_m, while the maximum C_n occurs when the vortex is over the mid-chord and the minimum C_m occurs when the vortex is over the trailing edge. Therefore, the timing of these important aerodynamic events depends upon the motion of the stall vortex.

The subject of the present paper is the convection speed of the dynamic stall vortex. This quantity has been measured by various researchers, and it emerges that alternative conclusions have been made as to the dependency of the convection speed upon the aerofoil motion. The following workers reported a dependency of convection speed upon aerofoil motion:

i) Carta [1] inferred the convection speed from a contour plot in time and space of the surface pressures measured on an oscillating NACA 0012.
ii) St. Hilaire & Carta [2] confirmed Carta's [1] results using the same measurement technique.
iii) Robinson & Luttges [3] performed oscillatory tests at lower Reynolds numbers than above and at higher reduced pitch rates. Convection speed was measured from flow visualisation results.
iv) Lorber & Carta [4] inferred the convection speed from the timing of suction peaks from measured surface pressure data.

Those works where the convection speed was found to be independent of aerofoil motion include the following:

i) Jumper et al. [5] inferred the convection speed from the delays in stall and separation incidences relative to the static case for ramp-up motions of a NACA 0015. Convection speed was found to be constant at 0.4U.
ii) Chandrasekhara & Carr [6] performed flow visualisation tests on a sinusoidally oscillating NACA 0012. They found that the convection speed was constant at 0.3U.
iii) Tuncer et al. [7] inferred the convection speed in the same way as Lorber & Carta [4] from pressure data from a solution of the Navier-Stokes equations at high Reynolds number and low Mach number for an oscillating NACA 0012. Convection speed was constant at 0.3U.

In addition to the above Galbraith et al. [8] used features on the surface pressure time histories to measure a dynamic stall duration for a variety of aerofoils. That work acted as a precursor to the present work. Table 1 shows a summary of the available data relating to the stall vortex convection speed. It can be seen that there is no particular pattern of blockage and aspect ratio to suggest a reason for the differing conclusions.

In this paper stall vortex convection speeds inferred from surface pressure data measured from several aerofoils performing various motion types are presented. Data from seven aerofoils were analysed for ramp-up, ramp-and-hold and oscillatory motions. The test facility and aerofoils are described together with the analysis technique. Results of the analysis are then presented and discussed. The work is described elsewhere in greater detail by Green et al. [9, 10].

2. THE UNIVERSITY OF GLASGOW DYNAMIC STALL TEST FACILITY

The general arrangement of the aerofoil in the wind tunnel is illustrated in figure 2. The test aerofoils, of chord length 0.55m and span 1.61m, were constructed of a fibre glass skin filled with epoxy resin foam and bonded to an aluminium spar. Each model was mounted vertically in the University of Glasgow's Handley-Page wind tunnel, which is a closed return type with a 1.61m x 2.13m octagonal working section. The aerofoil was pivoted about the quarter chord using a linear hydraulic actuator and crank mechanism.

Instantaneous aerofoil incidence was determined by a linear angular potentiometer geared to the model's tubular support. The dynamic pressure in the wind tunnel working section was obtained from the difference between the static pressure in the working section, 1.2m upstream of the leading edge, and the static pressure in the settling chamber, as measured by an electronic micromanometer. Thirty ultra-miniature pressure transducers were installed below the surface of the centre span of each aerofoil.

A series of experiments was performed on each aerofoil by rotating it about the quarter chord axis under four types of motion: steady, oscillatory (sinusoidal) and constant pitch rate ramp motions in both positive and negative directions. Oscillatory data was averaged over ten cycles, and the ramp data was averaged over five cycles. The effective free stream velocity was 40 ms^{-1} resulting in Reynolds and Mach numbers of 1.5 million and 0.11 respectively. The collected data were stored on a computer database. Figure 3 shows the aerofoil sections whose aerodynamic characteristics are considered in this report.

3. DATA ANALYSIS

Shown in figure 4 is a pseudo 3-D plot of the surface pressures measured from the NACA 23012C performing a ramp-up motion from -1^{o} to 40^{o} (a standard ramp-up test). When the pressures are plotted in this form, the passage of the stall vortex shows itself as a ridge (indicated in the figure). Early

measurements of the convection speed by Carta [1] were taken by measuring the gradient of the ridge line in time and space, and this was achieved by contour plotting the surface pressure plot. A criticism of this method is that it is not systematic, which may lead to subjective errors.

The contour plot/ ridge line technique has been superseded, however, by a more direct approach first described by Lorber & Carta [4]. As the stall vortex passes over the aerofoil surface, local suction peaks in the surface pressure distribution are formed. Thus, the passage of the stall vortex can be traced by measuring the timing of the suction peaks at each transducer position. Provided the pressure data is of adequate resolution, locating the suction peaks is a straightforward procedure. Shown in figure 5 are the chosen timing points on each of the individual pressure transducer traces. For the reduced pitch rate shown, the suction peaks are well defined, although for low reduced pitch rates and for thicker aerofoils the suction peaks can be quite weak and therefore difficult to locate accurately. Note that no timing points were used at the three trailing edge transducers; the reason for this is that as the vortex passes over the trailing edge an in-rush of air develops, and the last three transducers are indicating this rather than the stall vortex motion itself.

Figure 6 shows the stall vortex locus from figure 5. It is simply the chordwise location of the pressure transducer plotted against the non-dimensional time at which the suction peak occurred. The least squares straight line fit is excellent (correlation coefficient of 0.994), indicating that the convection speed is uniform across the chord, and the convection speed is equal to the gradient of the straight line. In this particular case u/U=0.36.

The above analysis technique was applied to the test aerofoils of figure 3. Results were obtained in the reduced pitch rate range $0.008<r<0.048$. The lower limit of this range was enforced by the vortex induced suction peaks becoming too poorly defined to give a reliable measurement of convection speed. Generally, the thicker the aerofoil, the higher the lower limit of the reduced pitch rate became. All the vortex speeds were measured over the last 80% of the chord, and the correlation coefficient of the straight line fit was always above 0.97.

4. RESULTS OF ANALYSIS

4.1 Standard ramp-up tests

Shown in figure 7 are the measured vortex convection speeds as a function of reduced pitch rate for the standard ramp-up tests for the seven test aerofoils. The level of scatter is large, but the 120 test cases shown indicate that the convection speed is independent of reduced pitch rate to a first order. Note that the mean convection speed for the NACA 0012 is significantly lower than for the other aerofoils. If the scatter is taken into account, however, the mean speeds are effectively the same as each other.

Also shown on this figure is the linear dependency found by Lorber & Carta [4]. Although their results were found at a lower reduced pitch rate range ($0.001<r<0.02$) than the present analysis, figure 7 strongly indicates that an anomaly exists between the two data sets.

4.2 Oscillatory aerofoil motion

The convection speed was measured from oscillatory motion tests in the same way as for the ramp-up tests. Analysis of the pressure data showed that the convection speed was uniform across the chord of the aerofoil. Figure 8 shows the variation of u/U as a function of reduced frequency for the NACA 23012C for pitch amplitudes of 10^{o} and 8^{o}. The amount of scatter is similar to the results from the ramp-up tests, and a similar conclusion is made to above, i.e. that the stall vortex convection speed is independent of reduced frequency to a first order.

4.3 Ramp-and-hold motion

A standard ramp-up test involves pitching the aerofoil from -1^{o} to 40^{o}. Ramp-and-hold tests were performed where the aerofoil was pitched from the same start incidence to above but held at a lower incidence, particularly at incidences such that the stall vortex would be convecting over a stationary aerofoil. These tests were performed on the NACA 0012 for a variety of reduced pitch rates. Table 2 shows the measured vortex convection speeds for the ramp-and-hold tests. Also shown on this table is the incidence at which the stall vortex is at x/c=0.17 for the 40^{o} hold angle for each reduced pitch rate. If this incidence is higher than the hold incidence, the vortex is convecting while the aerofoil is stationary.

On the whole, it can be seen that the hold incidence has little effect upon the convection speed. At very low hold incidence, however, the convection speeds appear to be higher. It was observed that as the hold incidence dropped, the strength of the vortex induced suction peaks also fell, with the result that the convection speed became difficult to measure. (This problem was also encountered as the reduced pitch rate decreased for the standard ramp-up tests.) The high values of u/U described above are the result of measurement difficulties and should not be regarded as a trend.

4.4 Analysis of unaveraged ramp-up data

The results discussed so far have related to the analysis of averaged data only: ramp-up tests were averaged over five cycles of motion, while oscillatory tests were averaged over ten. To check that the averaging of the data was not introducing any errors into the analysis, the unaveraged data from three ramp-up test cases for the NACA 0015 was analysed. Table 3 shows how the results of the analysis of the individual data sweeps compares with the averaged data. A point to note is that the mean of the results from the unaveraged data and the result of the averaged data are different. This difference is the inevitable consequence of slight phase differences of vortex motion between each data sweep. However, the results from the averaged data lie within the range of scatter from the unaveraged data, which indicates that the averaging process has not adversely affected the results of the convection speed.

4.5 Aerodynamic coefficients

As the reduced pitch rate increases, the dynamic increments to the aerodynamic coefficients and the stall incidence also increase. Table 4 shows how the incidences at maximum C_m and C_n along with the value of the coefficient vary with reduced pitch rate. Also shown on this table are the tendencies found by Lorber & Carta [4]. The increasing value of the coefficient in each case reflects the increase in strength of the stall vortex as reduced pitch rate increases, while the increasing incidence is the result of the pitch rate suppressing the stall. It is interesting to note that the results found by Lorber & Carta are similar to the present results.

5. DISCUSSION OF RESULTS

From the analysis of the Glasgow University data, it is concluded that the stall vortex convection speed is independent of the aerofoil motion to a first order. This is in direct contradiction to several works, particularly Lorber & Carta [4], in which it is asserted that the convection speed is dependent upon aerofoil motion. The discussion will concentrate upon the comparison with Lorber & Carta's work, as their test conditions most closely resemble those of the present work. An independent analysis of Lorber & Carta's data at the University of Glasgow confirmed their conclusions, so subtle differences in measurement technique are not the cause of the anomaly (Green et al. [10]). The relative agreement between the trends of the variation of the aerodynamic coefficients (table 4) is worth noting. It is expected that the aerodynamic coefficients and stall event incidences are pitch rate dependent, and the relative agreement indicates that essentially the same physical processes are occurring. The stall vortex strength and the delay in aerofoil stall ultimately relate to the behaviour of the attached flow, whereas the apparent convection speed anomaly concerns itself with the behaviour of the separated flow.

Lorber & Carta [11] suggested that the tendency is for the convection speed to be motion dependent at low reduced pitch rate and constant at high pitch rate. This is possible since Lorber & Carta's [4] results were found down to $r=0.001$, whereas the Glasgow University data applied at $r>0.008$. In an attempt to measure the convection speed at lower r, higher sampling frequencies were used for some ramp-up tests for the NACA 0012. The higher sampling frequency at low reduced pitch rate gave data of better resolution than in the standard tests, and allowed the stall vortex convection speed to be measured down to $r=0.006$. Lower than this reduced pitch rate and the stall vortex is far too weak. The results of the tests did not show the tendency suggested by Lorber & Carta [11], however, and merely reinforced our conclusion that the stall vortex convection speed is independent of aerofoil motion.

A further possibility is that the aerofoil type is important. Although this paper has described the analysis of seven aerofoils, they are all effectively of the same type, i.e. they exhibit trailing edge stall characteristics. The aerofoil tested by Lorber & Carta [4] was only 9% thick and had a sharp leading edge, resulting in leading edge stall characteristics. This raises the possibility that different aerofoils result in different vortex development and convection behaviour. Changes in vortex development are likely, although differences in actual vortex convection do not seem so plausible, since by the time the vortex starts to convect the shape of the aerofoil is made insignificant by the size of the separated zone. It may be possible that for some types of aerofoil, vortex development and convection are strongly intermingled. These thoughts, however, must remain as pure conjecture for the time being.

Finally, the problem of wind tunnel constraint must be discussed. Although table 1 does not show a pattern of blockage and aspect ratio that relates to the possible dependency of the convection speed upon aerofoil motion, when compared to Lorber & Carta's [4] model geometry the aspect ratio and blockage of the University of Glasgow models are a cause for concern. As yet no sufficient means for accounting for wind tunnel constraints in dynamic stall experiments exists, so the effects cannot be quantified. All that may be said for the time being is that the effect of constraint may alter the vortex trajectory, thereby affecting the perceived convection speed. It must be stressed that some of the test cases in table 1 were for blockage and aspect ratios considerably worse than for the University if Glasgow data. Carta [1] in particular

used a model and wind tunnel with a very low physical aspect ratio and high blockage, although the convection speed was found to be motion dependent. Although the effect of wind tunnel constraint does not appear to be specific from table 1, the comparison with the results of Lorber & Carta [4] strongly suggests that a study of wind tunnel constraint be made using the same experimental facility. To this effect, a NACA 0015 model of 0.275m chord is to be tested at the University of Glasgow. In addition it is recommended that cost effective computational techniques for dynamic stall prediction be developed. If the wind tunnel walls can be incorporated in the flow calculations, it is hoped that a good understanding of the effect of wind tunnel constraint can be gained.

6. CONCLUSIONS

An in depth analysis of dynamic stall data available on the G.U. database has shown that the stall vortex convection speed is independent of aerofoil motion to a first order. Specially designed tests served to reinforce this conclusion. Thus, a disharmony exists between the present work and the results of other workers, particularly Lorber & Carta [4], which is not the result of subtle differences in analysis technique.

The authors are indebted to the United States Air Force for the financing of the work under contract AFSOR 89-0397 A. Data collection was funded by the Science and Engineering Research Council, D.R.A. (Aerospace) and the Department of Energy.

REFERENCES

1. Carta, F.O. 'Analysis of Oscillatory Pressure Data Including Dynamic Stall Effects' **NASA CR** 2394 (1974)

2. St. Hilaire, A.O. & Carta, F.O. 'Analysis of Unswept and Swept Wing Pressure Data from an Oscillating NACA 0012 Airfoil Experiment.Volume I - Technical Report' **NASA CR** 3567 (1983)

3. Robinson, M.C. & Luttges, M.W. 'Unsteady Flow Separation and Attachment Induced by Pitching Aerofoils' **AIAA**-83-0131 (1983)

4. Lorber, P.F. & Carta, F.O. 'Unsteady Stall Penetration Experiments at High Reynolds Number' **AFOSR TR**-87-1202, **UTRC** R87-956939-3 (1987)

5. Jumper, E.J., Shreck, S.J. & Dimmick, R.L. 'Lift-curve Characteristics for an Aerofoil Pitching at Constant Rate' **AIAA**-86-0117 (1986)

6. Chandrasekhara, M. & Carr, L.W. 'Flow Visualisation Studies of the Mach Number Effects on the Dynamic Stall of an Aerofoil' **AIAA**-89-0023 (1989)

7. Tuncer, I.H., Wu, J.C. & Wang, C.M. 'Theoretical and Numerical Studies of Oscillating Aerofoils' **AIAA Journal 28**, 1615 (1990)

8. Galbraith, R.A.McD., Niven, A.J. & Seto, L.Y. 'On the Duration of Low Speed Dynamic Stall' **Proceedings of the 15th ICAS Conference, London** (1986)

9. Green, R.B., Galbraith, R.A.McD. & Niven, A.J. 'Measurements of the Dynamic Stall Vortex Convection Speed' **AFOSR** Contract N° 89-0397 A, **University of Glasgow, Dept. Aerospace Engineering,** Report N° 9014 (1990)

10. Green, R.B., Galbraith, R.A.McD. & Niven, A.J. 'The Dynamic Stall Vortex Convection Speed Anomaly: Analysis of Lorber & Carta's Pressure Data' **AFOSR** Contract N° 89-0397 A, **University of Glasgow, Dept. Aerospace Engineering,** Report N° 9101 (1991)

11. Lorber, P.F. & Carta, F.O. **Private Communication** (1991)

TABLE 1

Test conditions for measurements of stall vortex convection speed.

Author	Aerofoil	Re.	M	AR	c/h	Ramp	Sine	Range of k or r. Variation of wave speed
Carta (1974)	NACA 0012	$1x10^6$	0.35	9.5 0.8	0.28	-	$\hat{\alpha}=8^o$ $\bar{\alpha}=3^o-18^o$	0 - 0.4, increasing
St. Hilaire & Carta (1983)	NACA 0012	$2.8x10^6$	0.3	6.1	0.163	-	$\hat{\alpha}=8^o$ $\bar{\alpha}$ up to 15^o	0 - 0.12, increasing
Lorber & Carta (1987)	SSC-A09	$2-4x10^6$	0.2-0.4	5.56	0.18	up to 30^o	$\hat{\alpha}=10^o, 20^o$ $\bar{\alpha}=10^o$	sine: 0.025 - 0.1 ramp: 0.005-0.02 increasing
Chandrasekhara & Carr (1983)	NACA 0012	$2-9x10^5$	0.15-0.45	3.33	0.214	-	$\hat{\alpha}=10^o$ $\bar{\alpha}=10^o$	0 - 0.1, constant
Galbraith et al (1986)	NACA23012 23012A	$1.5x10^6$	0.12	2.93	0.26	-1^o to 40^o	$\hat{\alpha}=10^o$ $\bar{\alpha}=15^o$	sine: - 0.24 constant time ramp: 0.045 delay
Robinson & Luttges (1983)	NACA 0012	$6-14x10^4$	<0.024	2.4	0.417	-	$\hat{\alpha}$ up to 5^o $\bar{\alpha}=13^o-15^o$	0.25 - 0.75, increasing
Jumper et al (1986)	NACA 0015	$1.58-2.81$ $x10^6$	<0.038	2.94	0.204	up to 40^o	-	0.01 - 0.03, constant

TABLE 2: Ramp-and-hold convection speed data for the NACA 0012

Reduced Pitch Rate	Hold Incidence (deg)	Convection Speed (u/U)	Incidence at which vortex is at x/c=0.17
0.03907	40	0.28	29.8
0.04162	30	0.28	held
0.04009	26	0.29	held
0.03750	22	0.31	held
0.03700	40	0.26	29.5
0.03892	30	0.29	held
0.03664	26	0.31	held
0.03634	22	0.31	held
0.03556	40	0.29	28.8
0.03527	30	0.30	29.0
0.03458	26	0.29	held
0.03315	22	0.35	held
0.02645	40	0.27	27.2
0.02676	30	0.26	27.0
0.02663	26	0.27	held
0.02930	22	0.35	held
0.02179	40	0.32	27.0
0.02285	25	0.31	held
0.02188	22	0.40	held
0.01686	40	0.28	25.1
0.01685	25	0.29	held
0.01626	22	0.32	held
0.01265	40	0.31	24.0
0.01348	25	0.26	held
0.01398	22	0.37	held

TABLE 3: Comparison of convection speeds from averaged and unaveraged data (NACA 0015, ramp-up motion)

reduced pitch rate	stall vortex convection speed (u/U)		
	results from unaveraged data	average of unaveraged	result from averaged data
0.036	0.37, 0.35, 0.33, 0.35, 0.29	0.34	0.36
0.035	0.35, 0.30, 0.34, 0.39, 0.34	0.34	0.35
0.034	0.38, 0.31, 0.34, 0.39, 0.39	0.36	0.32

TABLE 4

Variation of aerodynamic coefficients with reduced pitch rate

Aerofoil	Gradients of straight line fits (dependence upon r)				
	α at max C_n	max C_n	α at max C_m	max C_m	α at C_n rise
NACA 23012	526	39	549	-8	296
NACA 23012A	496	67	612	-14	
NACA 23012B	457	55	441	-17	
NACA 23012C	502	61	527	-19	
NACA 0012	451	26	480	-11	
NACA 0015	507	83	612	-20	
NACA 0018	538	74	511	-22	
Lorber & Carta	500 (C_L)	40 (C_L)	550	-18	192 (C_L)

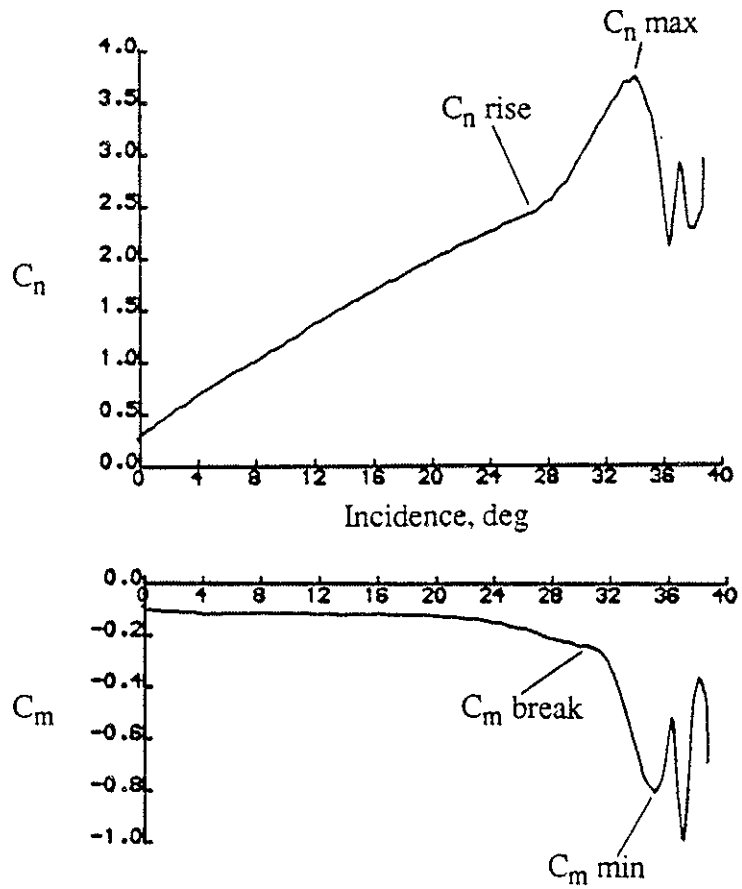

Figure 1. C_n and C_m as a function of incidence for the NACA 23012C performing a ramp-up motion from -1° to 40° at r=0.032. The salient features are indicated.

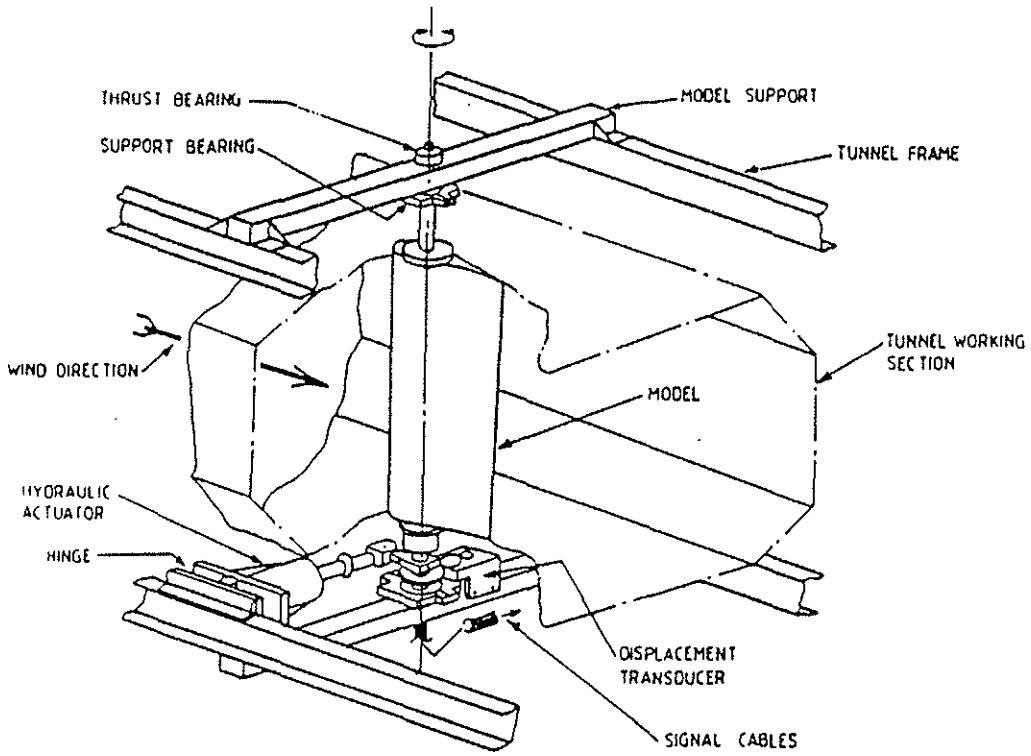

Figure 2. The wind tunnel working section with the unsteady aerofoil test apparatus.

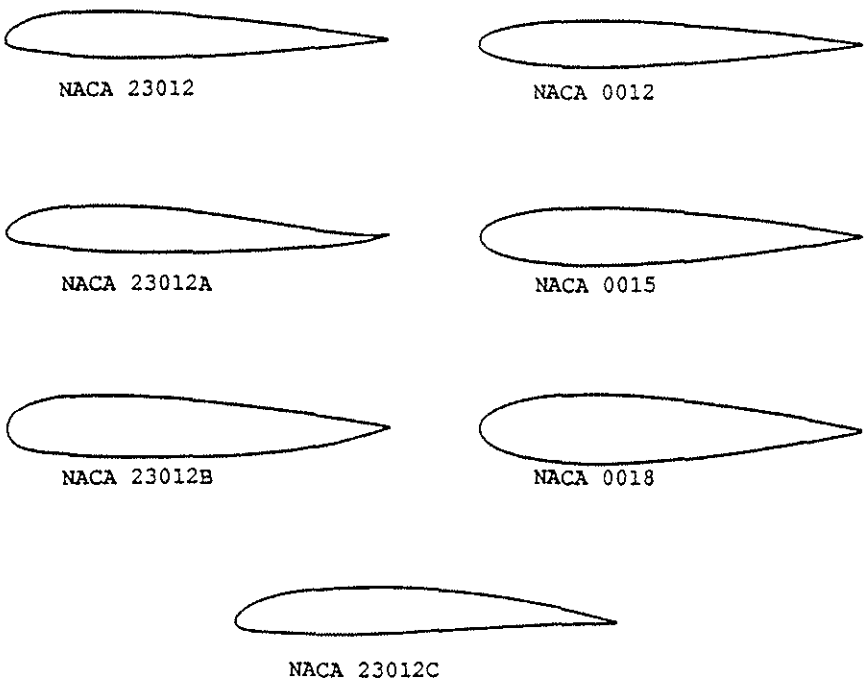

Figure 3. Test aerofoil sections.

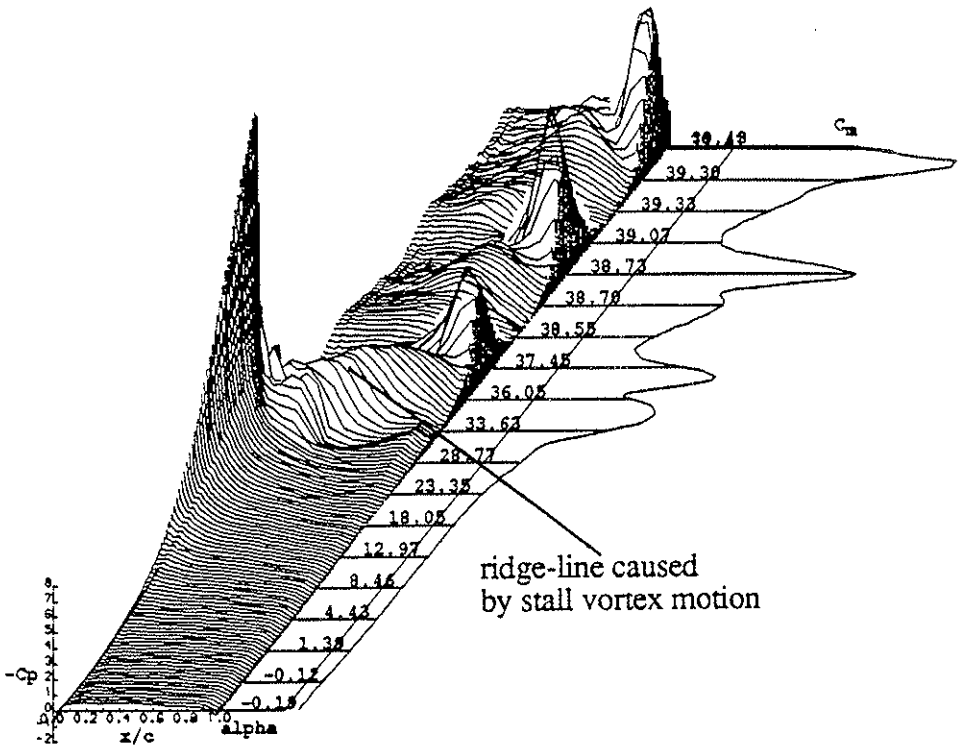

Figure 4. Pseudo-3-D surface pressure plot showing the development of the pressures on the aerofoil surface with incidence. The passage of the stall vortex appearsas a ridge as indicated. Test conditions as for figure 1.

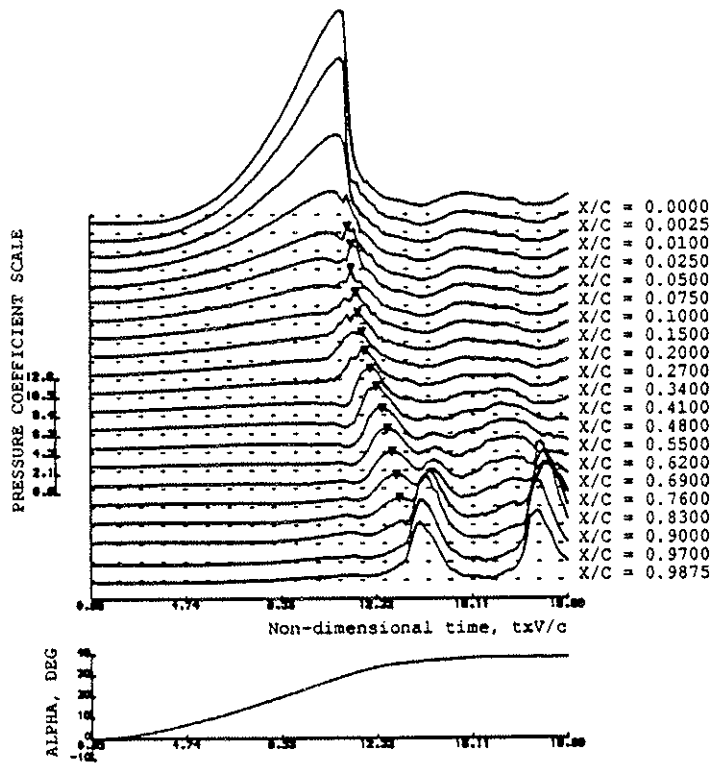

Figure 5. Individual surface pressure transducer traces plotted as a function of time. The suction peaks induced by the stall vortex are indicated by the symbols. Test conditions as for figure 1.

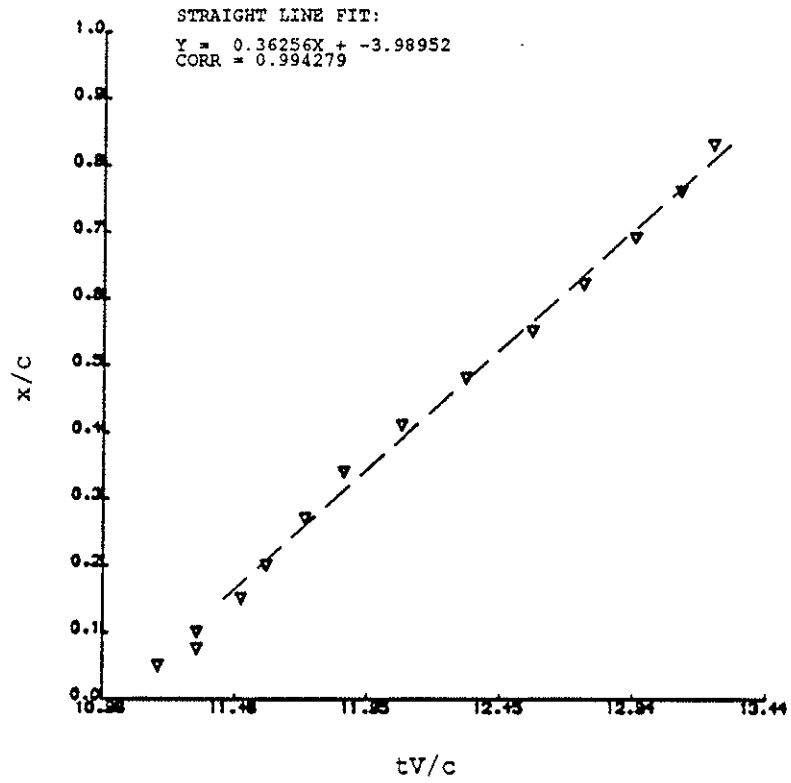

Figure 6. Stall vortex position vs time. Test conditions as for figure 1

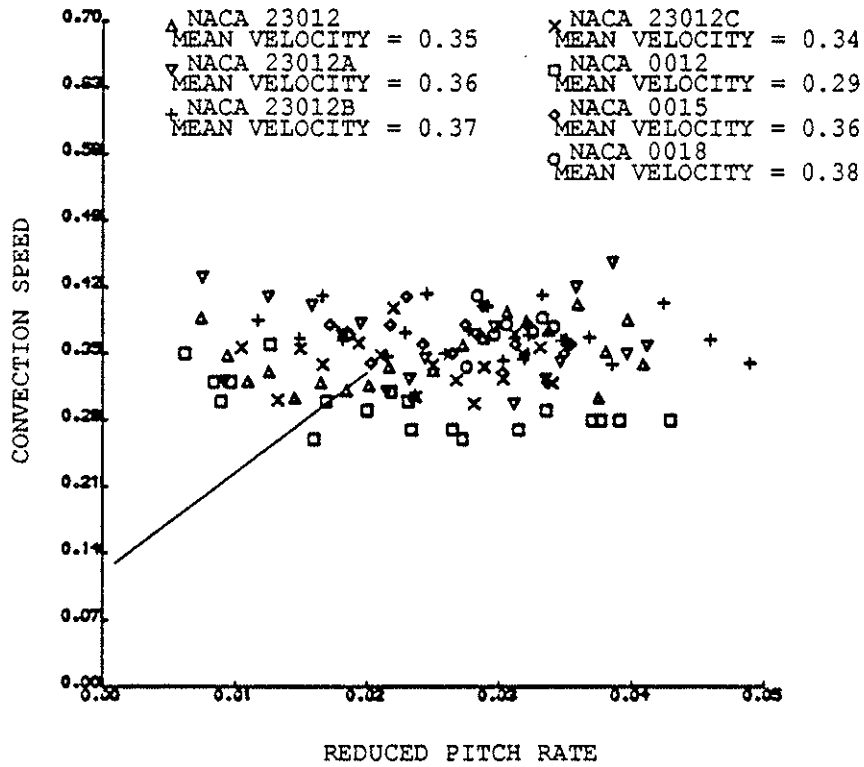

Figure 7. The collected stall vortex convection speed data for ramp-up motion. Lorber & Carta's result is shown by the solid line.

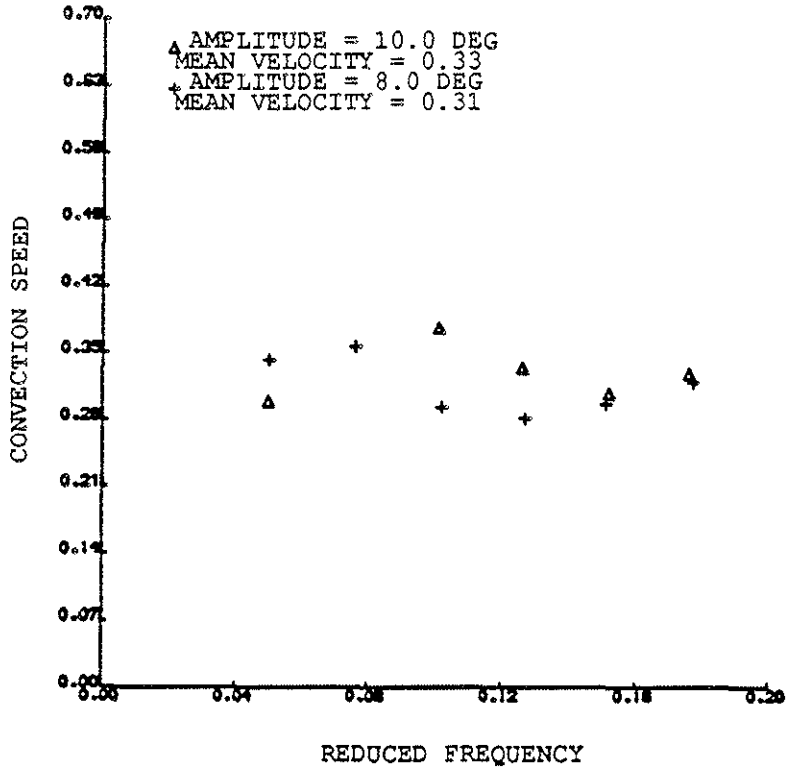

Figure 8. Stall vortex convection speed as a function of reduced frequency for the NACA 23012C.